

## Search for the Blazhko effect in field RR Lyrae stars using LINEAR and ZTF light curves

2 EMA DONEV<sup>1</sup> AND ŽELJKO IVEZIĆ<sup>2</sup>

3 <sup>1</sup>*XV. Gymnasium (MIOC), Jordanovac 8, 10000, Zagreb, Croatia*

4 <sup>2</sup>*Department of Astronomy and the DiRAC Institute, University of Washington, 3910 15th Avenue NE, Seattle, WA 98195, USA*

### 5 ABSTRACT

6 We analyzed the incidence and properties of RR Lyrae stars that show evidence for amplitude and  
7 phase modulation (the so-called Blazhko Effect) in a sample of  $\sim$ 3,000 stars with LINEAR and ZTF  
8 light curve data collected during the periods of 2002–2008 and 2018–2023, respectively. A preliminary  
9 subsample of about  $\sim$ 500 stars was algorithmically pre-selected using various data quality and light  
10 curve statistics, and then 228 stars were confirmed visually as displaying the Blazhko effect. This  
11 sample increases the number of field RR Lyrae stars displaying the Blazhko effect by more than 50%  
12 and places a lower limit of  $(11.4 \pm 0.8)\%$  for their incidence rate. We find that ab type RR Lyrae  
13 that show the Blazhko effect have about 5% (0.030 day) shorter periods than starting sample, a  $7.1\sigma$   
14 statistically significant difference. We find no significant differences in their light curve amplitudes and  
15 apparent magnitude (essentially, signal-to-noise ratio) distributions. No period or other differences are  
16 found for c type RR Lyrae. We find convincing examples of stars where the Blazhko effect can appear  
17 and disappear on time scales of several years. With time-resolved photometry expected from LSST, a  
18 similar analysis will be performed for even larger samples of fields RR Lyrae stars in the southern sky  
19 and we anticipate a higher fraction of discovered Blazhko stars due to better sampling and superior  
20 photometric quality.

21 **Keywords:** Variable stars — RR Lyrae variable stars — Blazhko effect

### 22 1. INTRODUCTION

23 RR Lyrae stars are pulsating variable stars with per-  
24 iodis in the range of 3–30 hours and large amplitudes that  
25 increase towards blue optical bands (e.g., in the SDSS *g*  
26 band from 0.2 mag to 1.5 mag; Sesar et al. 2010). For  
27 comprehensive reviews of RR Lyrae stars, we refer the  
28 reader to Smith (1995) and Catelan (2009).

29 RR Lyrae stars often exhibit amplitude and phase  
30 modulation, or the so-called Blazhko effect<sup>1</sup> (hereafter,  
31 “Blazhko stars”). For examples of well-sampled observed  
32 light curves showing the Blazhko effect, see, e.g., Ke-  
33 pler data shown in Figures 1 and 2 from Benkő et al.  
34 (2010). The Blazhko effect has been known for a long  
35 time (Blažko 1907), but its detailed observational prop-  
36 erties and theoretical explanation of its causes remain  
37 elusive (Kolenberg 2008; Kovács 2009; Szabó 2014). Var-  
38 ious proposed models for the Blazhko effect, and prin-  
39 cipal reasons why they fail to explain observations, are  
40 summarized in Kovacs (2016).

Corresponding author: Željko Ivezić  
ivezic@uw.edu

<sup>1</sup> The Blazhko effect was discovered by Lidiya Petrovna Tseraskaya and first reported by Sergey Blazhko.

41 A part of the reason for the incomplete observational  
42 description of the Blazhko effect is difficulties in discov-  
43 ering a large number of Blazhko stars due to tempo-  
44 ral baselines that are too short and insufficient number  
45 of observations per object (Kovacs 2016; Hernitschek &  
46 Stassun 2022). With the advent of modern sky sur-  
47 veys, several studies reported large increases in the num-  
48 ber of known Blazhko stars, starting with a sample of  
49 about 700 Blazhko stars discovered by the MACHO sur-  
50 vey towards the LMC (Alcock et al. 2003) and about  
51 500 Blazhko stars discovered by the OGLE-II survey  
52 towards the Galactic bulge (Mizerski 2003). Most re-  
53 cently, about 4,000 Blazhko stars were discovered in the  
54 LMC and SMC (Soszyński et al. 2009, 2010), and an  
55 additional  $\sim$ 3,500 stars were discovered in the Galactic  
56 bulge (Soszyński et al. 2011; Prudil & Skarka 2017), both  
57 by the OGLE-III survey. Nevertheless, discovering the  
58 Blazhko effect in field RR Lyrae stars that are spread  
59 over the entire sky remains a much harder problem: only  
60 about 400 Blazhko stars in total (Skarka 2013) from all  
61 the studies of field RR Lyrae stars have been reported  
62 so far (see also Table 1 in Kovacs 2016).

63 Here, we report the results of a search for the Blazhko  
64 effect in a sample of  $\sim$ 3,000 field RR Lyrae stars with  
65 LINEAR and ZTF light curve data. A preliminary sub-

sample of about  $\sim 500$  stars was selected using various light curve statistics, and then 228 stars were confirmed visually as displaying the Blazhko effect. This new sample doubles the number of field RR Lyrae stars that exhibit the Blazhko effect. In §2 and §3 we describe our datasets and analysis methodology, and in §4 we present our analysis results. Our main results are summarized and discussed in §5.

74

## 75 2. DATA DESCRIPTION AND PERIOD 76 ESTIMATION

77 Analysis of field RR Lyrae stars requires a sensitive  
78 time-domain photometric survey over a large sky area.  
79 For our starting sample, we used  $\sim 3,000$  field RR Lyrae  
80 stars with light curves obtained by the LINEAR aster-  
81 oid survey. In order to study long-term changes in light  
82 curves, we also utilized light curves obtained by the ZTF  
83 survey which monitored the sky  $\sim 15$  years after LIN-  
84 EAR. The combination of LINEAR and ZTF provided  
85 a unique opportunity to systematically search for the  
86 Blazhko effect in a large number of field RR Lyrae stars  
87 over a large time span of two decades.

88 We first describe each dataset in more detail, and then  
89 introduce our analysis methods. All our analysis code,  
90 written in Python, is available on GitHub<sup>2</sup>.

91

### 2.1. LINEAR Dataset

92 The properties of the LINEAR asteroid survey and  
93 its photometric re-calibration based on SDSS data are  
94 discussed in Sesar et al. (2011). Briefly, the LINEAR  
95 survey covered about  $10,000 \text{ deg}^2$  of the northern sky  
96 in white light (no filters were used, see Fig. 1 in Sesar  
97 et al. 2011), with photometric errors ranging from  $\sim 0.03$   
98 mag at an equivalent SDSS magnitude of  $r = 15$  to  $0.20$   
99 mag at  $r \sim 18$ . Light curves used in this work include,  
100 on average, 270 data points collected between December  
101 2002 and September 2008.

102 A sample of 7,010 periodic variable stars with  $r < 17$   
103 discovered in LINEAR data were robustly classified by  
104 Palaversa et al. (2013), including about  $\sim 3,000$  field RR  
105 Lyrae stars of both ab and c type, detected to distances  
106 of about 30 kpc (Sesar et al. 2013). The sample used  
107 in this work contains 2196 ab-type and 745 c-type RR  
108 Lyrae, selected using classification labels and the *gi* color  
109 index from Palaversa et al. (2013). The LINEAR light  
110 curves, augmented with IDs, equatorial coordinates, and  
111 other data, were accessed using the astroML Python  
112 module<sup>3</sup> (VanderPlas et al. 2012).

113

### 2.2. ZTF Dataset

<sup>2</sup> [https://github.com/emadonev/var\\_stars](https://github.com/emadonev/var_stars)

<sup>3</sup> For an example of light curves, see [https://www.astroml.org/book\\_figures/chapter10/fig\\_LINEAR\\_LS.html](https://www.astroml.org/book_figures/chapter10/fig_LINEAR_LS.html)

114 The Zwicky Transient Factory (ZTF) is an opti-  
115 cal time-domain survey that uses the Palomar 48-inch  
116 Schmidt telescope and a camera with  $47 \text{ deg}^2$  field of  
117 view (Bellm et al. 2019). The dataset analyzed here  
118 was obtained with SDSS-like *g*, *r*, and *i* band filters.  
119 Light curves for objects in common with the LINEAR  
120 RR Lyrae sample typically have smaller random photo-  
121 metric errors than LINEAR light curves because ZTF  
122 data are deeper (compared to LINEAR, ZTF data have  
123 about 2-3 magnitudes fainter  $5\sigma$  depth). ZTF data used  
124 in this work were collected between February 2018 and  
125 December 2023, on average about 15 years after obtain-  
126 ing LINEAR data. The median number of observations  
127 per star for ZTF light curves is  $\sim 500$ .

128 The ZTF dataset for this project was created by se-  
129 lecting ZTF IDs with matching equatorial coordinates to  
130 a corresponding LINEAR ID of an RR Lyrae star. This  
131 process used the *ztfquery* function, which searched the  
132 coordinates in the ZTF database within 3 arcsec from  
133 the LINEAR position. The resulting sample consisted of  
134 2857 RR Lyrae stars with both LINEAR and ZTF data.  
135 The fractions of RRab and RRc type RR Lyrae in this  
136 sample, 71% RRab and 29% RRc type, are consistent  
137 with results from other surveys (e.g., Sesar et al. 2010).

138

### 2.3. Period Estimation

139 The first step of our analysis is estimating best-fit peri-  
140 ods, separately for LINEAR and ZTF datasets. We used  
141 the Lomb-Scargle method (Vanderplas 2015) as imple-  
142 mented in *astropy* (Astropy Collaboration et al. 2018).  
143 The period estimation used 3 Fourier components and  
144 a two-step process: an initial best-fit frequency was de-  
145 termined using the *autopower* frequency grid option and  
146 then the power spectrum was recomputed around the  
147 initial frequency using an order of magnitude smaller  
148 frequency step. In case of ZTF, we estimated period  
149 separately for each available passband and adopted their  
150 median value. Once the best-fit period was determined,  
151 a best-fit model for the phased light curve was computed  
152 using 6 Fourier components. Fig 1 shows an example of  
153 a star with LINEAR and ZTF light curves, phased light  
154 curves, and their best-fit models.

155 We found excellent agreement between the best-fit  
156 periods estimated separately from LINEAR and ZTF  
157 light curves. The median of their ratio is unity within  
158  $2 \times 10^{-6}$  and the robust standard deviation of their ratio  
159 is  $2 \times 10^{-5}$ . With a median sample period of 0.56 days,  
160 the implied scatter of period difference is about 1.0 sec.

161 Given on average about 15 years between LINEAR  
162 and ZTF data sets, and a typical period of 0.56 days,  
163 this time difference corresponds to about 10,000 oscilla-  
164 tions. With a fractional period uncertainty of  $2 \times 10^{-5}$ ,  
165 LINEAR data can predict the phase of ZTF light curve  
166 with an uncertainty of 0.2. Therefore, for a robust de-  
167 tection of light curve phase modulation, each data set  
168 must be analyzed separately. On the other hand, ampli-

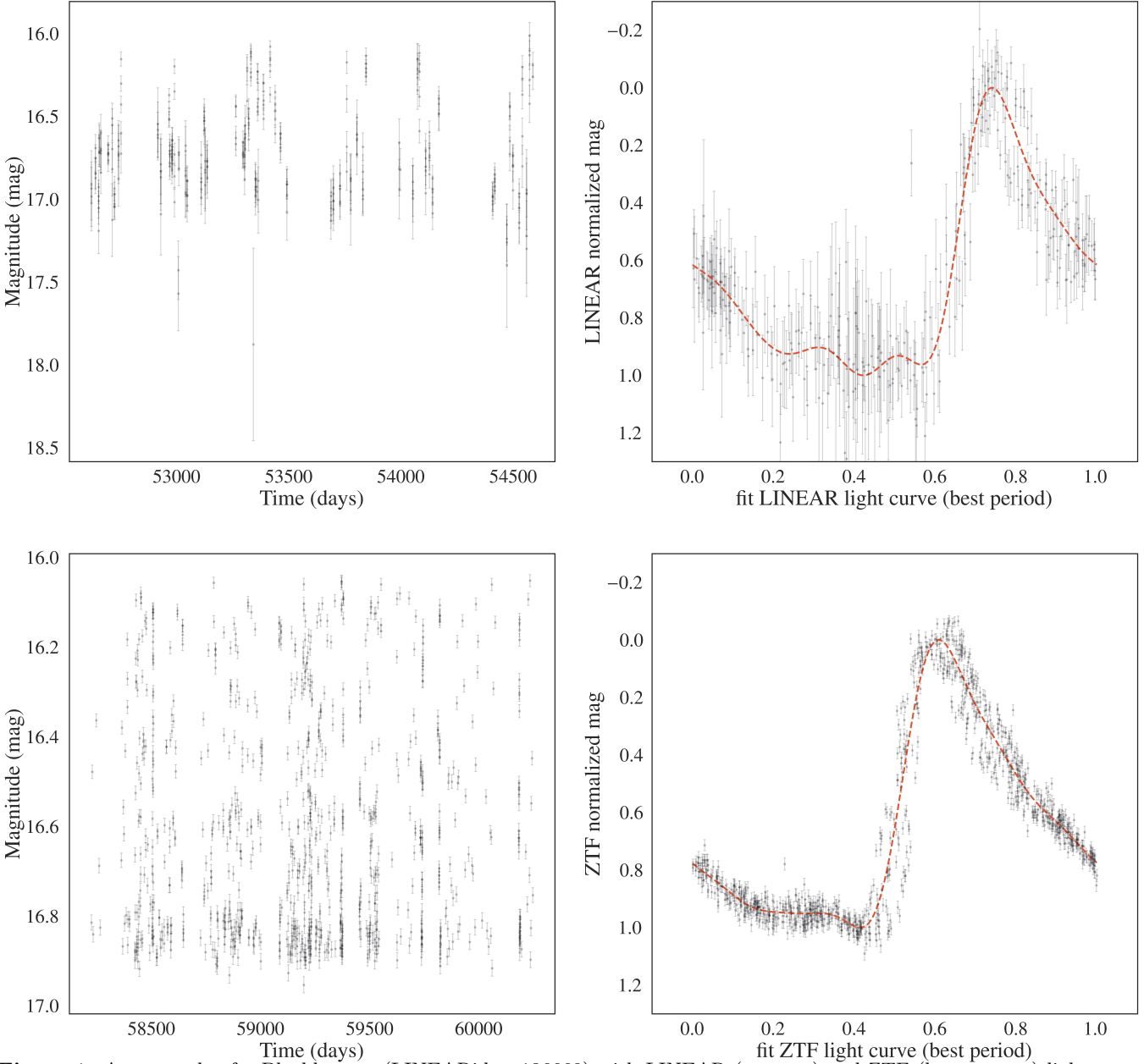


**Figure 1.** An example of a Blazhko star (LINEARid = 136668) with LINEAR (top row) and ZTF (bottom row) light curves (left panels, data points with “error bars”), phased light curves normalized to the 0–1 range (right panels, data points with “error bars”), with their best-fit models shown by dashed lines. The best-fit period is determined for each dataset separately using 3 Fourier terms. The models shown in the right panels are evaluated with 6 Fourier terms.

tude modulation can be detected on time scales as long as 15 years, as discussed in the following section.

### 3. ANALYSIS METHODOLOGY: SEARCHING FOR THE BLAZHKO EFFECT

Given the two sets of light curves from LINEAR and ZTF, we searched for amplitude and phase modulation, either during the 5–6 years of data taking by each survey, or during the average span of 15 years between the two surveys. Starting with a sample of 2857 RR Lyrae stars, we pre-selected a smaller sample that was

inspected visually (see below for details). We also required at least 150 LINEAR data points and 150 ZTF data points (for the selected band from which we calculated the period) in analyzed light curves. We used two pre-selection methods that are sensitive to different types of light curve modulation: direct light curve analysis and periodogram analysis, as follows.

#### 3.1. Direct Light Curve Analysis

Given statistically correct period, amplitude and light curve shape estimates, as well as data being consistent

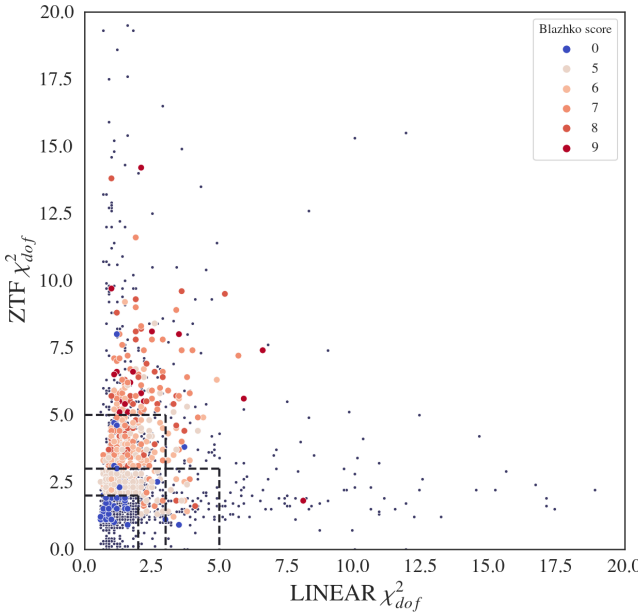


**Figure 2.** A selection diagram constructed with the two sets of robust  $\chi^2_{dof}$  values, for LINEAR and ZTF data sets, where the dark blue dots represent all RR Lyrae stars and the circles represent candidate Blazhko stars (color-coded according to the legend, with B\_score representing the number of points scored from the selection algorithm). The horizontal and vertical dashed lines help visualize selection boundaries for Blazhko candidates (see text).

with reported (presumably Gaussian) uncertainty estimates, the  $\chi^2$  per degree of freedom gives a quantitative assessment of the "goodness of fit",

$$\chi^2_{dof} = \frac{1}{N_{dof}} \sum \frac{(d_i - m_i)^2}{\sigma_i^2}. \quad (1)$$

Here,  $d_i$  are measured light curve data values at times  $t_i$ , and with associated uncertainties  $\sigma_i$ ,  $m_i$  are best-fit models at times  $t_i$ , and  $N_{dof}$  is the number of degrees of freedom, essentially the number of data points. In the absence of any light curve modulation, the expected value of  $\chi^2_{dof}$  is unity, with a standard deviation of  $\sqrt{2/N_{dof}}$ . If  $\chi^2_{dof} - 1$  is many times larger than  $\sqrt{2/N_{dof}}$ , it is unlikely that data  $d_i$  were generated by the assumed (unchanging) model  $m_i$ . Of course,  $\chi^2_{dof}$  can also be large due to underestimated measurement uncertainties  $\sigma_i$ , or to occasional non-Gaussian measurement error (the so-called outliers).

Therefore, to search for signatures of the Blazhko effect, manifested through statistically unlikely large values of  $\chi^2_{dof}$ , we computed  $\chi^2_{dof}$  separately for LINEAR and ZTF data (see Fig. 2). Using the two sets of  $\chi^2_{dof}$  values, we algorithmically pre-selected a sample of candidate Blazhko stars for further visual analysis of their light curves. The visual analysis is needed to confirm the expected Blazhko behavior in observed light curves,

as well as to identify cases of data problems, such as photometric outliers.

We used a simple scoring algorithm, optimized through trial and error, that utilized the two values of  $\chi^2_{dof}$ , augmented by period and amplitude differences, as follows. A star could score a maximum of 9 points, and a minimum of 5 points was required for further visual analysis. The  $\chi^2_{dof}$  selection boundaries are illustrated in Fig. 2. If either value of  $\chi^2_{dof}$  exceeded 5, or both exceeded 3, a star was awarded 5 points and immediately selected for further analysis. If these  $\chi^2_{dof}$  criteria were not met, a star could still be selected by meeting less stringent  $\chi^2_{dof}$  selection if it also had large period or amplitude difference between LINEAR and ZTF datasets. Stars with at least one value of  $\chi^2_{dof}$  above 2 would receive 3 points and those with at least one  $\chi^2_{dof}$  above 3 would receive 4 points. A period difference exceeding  $2 \times 10^{-4}$  day would be awarded 1 point and two points for exceeding  $5 \times 10^{-4}$  day. Analogous limits for amplitude difference were 0.05 mag and 0.15 mag, respectively.

The candidate Blazhko sample pre-selected using this method includes 531 stars. For most selected stars, the  $\chi^2_{dof}$  values were larger for the ZTF data because the ZTF photometric uncertainties are smaller than for the LINEAR data set. Fig. 3 summarizes the selection criteria and the resulting numbers of selected stars for each criterion and their combinations.

### 3.2. Periodogram Analysis

When light curve modulation is due to double-mode oscillation with two similar oscillation frequencies (periods), it is possible to recognize its signature in the periodogram computed as part of the Lomb-Scargle analysis. Depending on various details, such as data sampling and the exact values of periods, amplitudes, this method may be more efficient than direct light curve analysis (Skarka et al. 2020). We also employed this method to select additional candidates, as follows.

A sum of two *sine* functions with same amplitudes and with frequencies  $f_1$  and  $f_2$  can be rewritten using trigonometric equalities as

$$y(t) = 2 \cos(2\pi \frac{f_1 - f_2}{2} t) \sin(2\pi \frac{f_1 + f_2}{2} t). \quad (2)$$

We can define

$$f_o = \frac{f_1 + f_2}{2}, \quad (3)$$

and

$$\Delta f = \left| \frac{f_1 - f_2}{2} \right|, \quad (4)$$

with  $\Delta f \ll f_o$  when  $f_1$  and  $f_2$  are similar. The fact that  $\Delta f$  is much smaller than  $f_o$  means that the period of the *cos* term is much larger than the period of the basic oscillation ( $f_o$ ). In other words, the *cos* term acts as a slow amplitude modulation of the basic oscillation. When the amplitudes of two *sine* functions are

### Analysis of blazhko star metrics for RR Lyrae

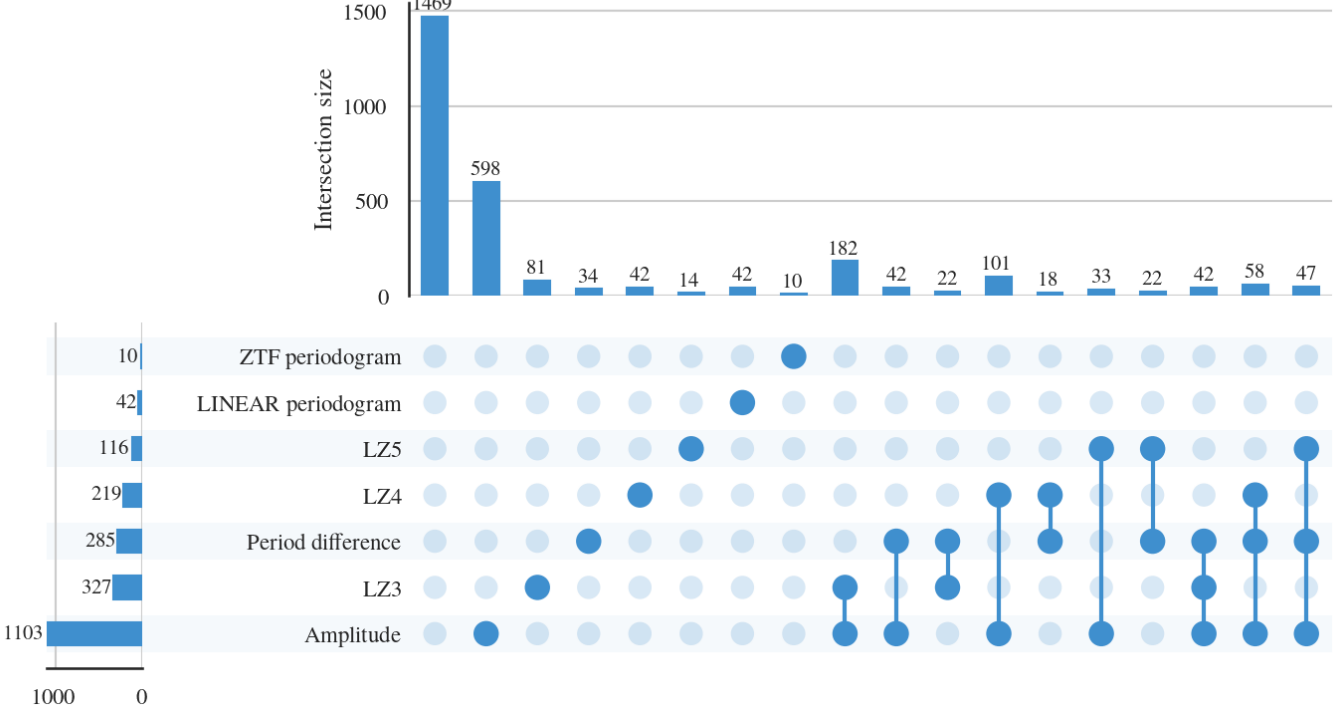


**Figure 3.** The figure shows selection criteria and the resulting numbers of pre-selected Blazhko star candidates for each criterion and their combinations (x in LZx corresponds to the number of scored points in the  $\chi^2_{dof}$  vs.  $\chi^2_{dof}$  diagram (see Fig. 2). The dots represent each case a star can occupy, where every solid dot is a specific criterion that is satisfied. Connections between solid dots represent stars which satisfy multiple criteria. Each dot combination has its own count, represented by the horizontal countplot. The vertical countplot shows the total number of stars that satisfy one criteria (union of all cases). For example, a total of 116 stars passed the LZ5 criterion, with 14 of them satisfying only  $\chi^2$  criterion, 33 also had a significant amplitude change, 22 had a significant period difference, and 47 had both a significant period and amplitude difference along with the satisfied  $\chi^2$  criterion. The sum of all specific cases is 116.

not equal, the results are more complicated but the basic conclusion about amplitude modulation remains. When the power spectrum of  $y(t)$  is constructed, it will show 3 peaks: the main peak at  $f_o$  and two more peaks at frequencies  $f_o \pm \Delta f$ . We used this fact to construct an algorithm for automated searching for the evidence of amplitude modulation. Fig 4 compares the theoretical periodogram produced by interference beats with our algorithm's periodogram, signifying that local Blazhko peaks are present in real data.

After the strongest peak in the Lomb-Scargle periodogram is found at frequency  $f_o$ , we search for two equally distant local peaks at frequencies  $f_-$  and  $f_+$ , with  $f_- < f_o < f_+$ . The sideband peaks can be highly asymmetric Alcock et al. (2003) and observed periodograms can sometimes be much more complex Szczygieł & Fabrycky (2007). We fold the periodogram through the main peak at  $f_o$ , multiply the two branches and then search for the strongest peaks in the resulting folded periodogram that is statistically more significant than the background noise. The background noise is computed as the scatter of the folded periodogram

estimated from the interquartile range. We require a “signal-to-noise” ratio of at least 5, as well as the peak strength of at least 0.05 for ZTF, while 0.10 for LINEAR data. If such a peak is found, and it doesn't correspond to yearly alias, we select the star as a candidate Blazhko star and compute its Blazhko period as

$$P_{BL} = |f_{-,+} - f_o|^{-1},$$

where  $f_{-,+}$  means the Blazhko sideband frequency with a higher amplitude is chosen.

The observed Blazhko periods range from 3 to 3,000 days, and Blazhko amplitudes range from 0.01 mag to about 0.3 mag (Szczygieł & Fabrycky 2007). In this work, we selected a smaller Blazhko range due to the limitations of our data: 30–325 days. With this additional constraint, we selected 52 candidate Blazhko stars. Fig. 4 shows an example where two very prominent peaks were identified in the LINEAR periodogram.

#### 3.2.1. Visual Confirmation

The sample pre-selected for visual analysis includes 531 RR Lyrae stars ( $479 + 52$ ), or 18.1% of the starting

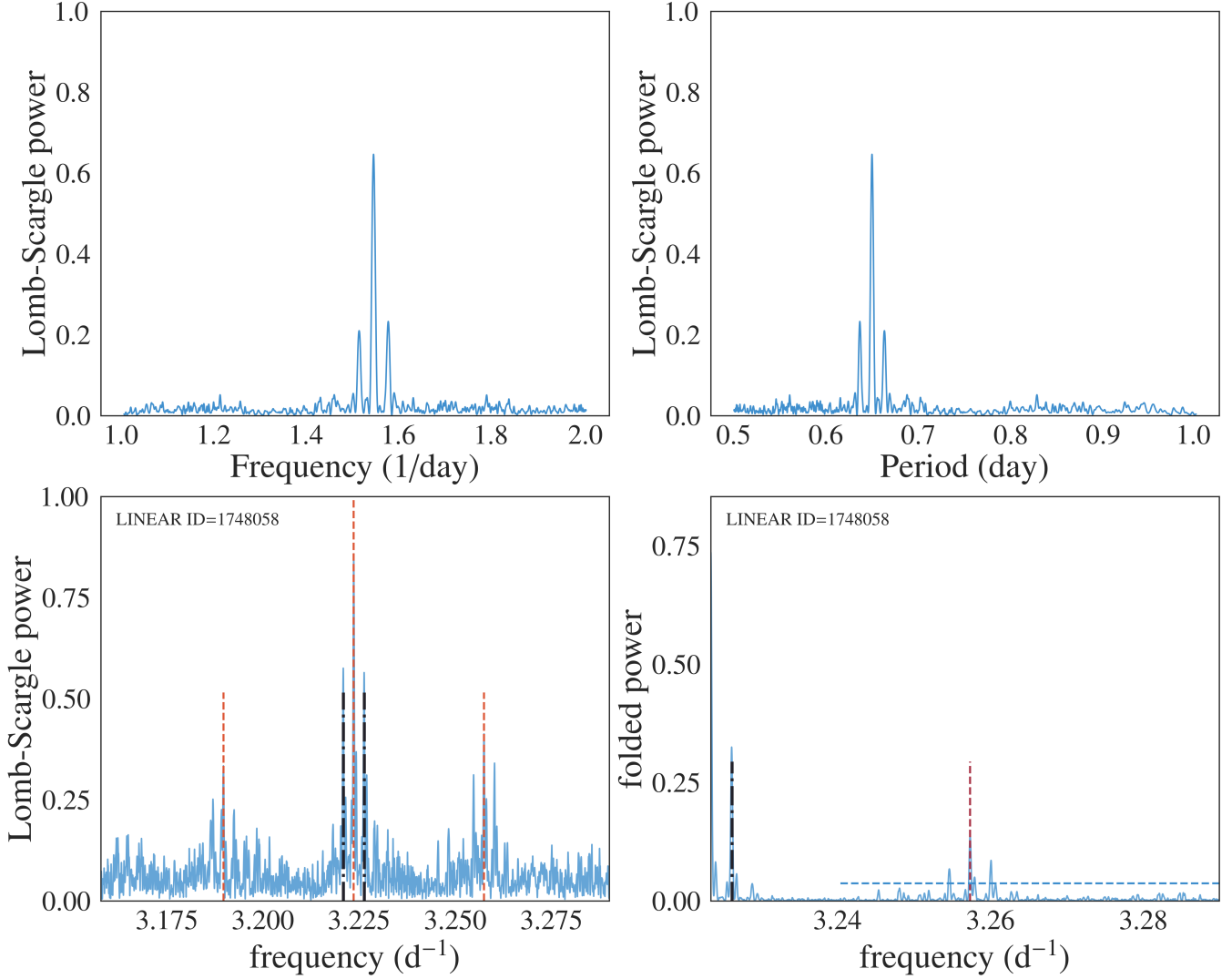


**Figure 4.** The top two panels show a simulated periodogram for a sum of two *sine* functions with similar frequencies  $f_1$  and  $f_2$  – the central peak corresponds to their mean (see eqs. 3 and 4). The bottom left panel shows a periodogram for an observed LINEAR light curve for  $ID = 1748058$ , and the bottom right panel shows its folded version (around the main frequency  $f_o = 3.223 \text{ d}^{-1}$ ). In the bottom left panel, the three vertical dashed lines show the three frequencies identified by the algorithm described in text, and the two dot-dashed lines mark yearly aliases around the main frequency  $f_o$ , at frequencies  $f_o \pm 0.0274 \text{ d}^{-1}$ . The two vertical lines in the bottom right panel have the same meaning, and the horizontal dashed line shows the noise level multiplied by 5.

306 LINEAR-ZTF sample. Visual analysis included the fol-  
307 lowing standard steps (e.g., Jurcsik et al. 2009; Prudil  
308 & Skarka 2017):

- 309 1. The shape of the phased light curves and scatter of  
310 data points around the best-fit model were exam-  
311 ined for signatures of anomalous behavior indica-  
312 tive of the Blazhko effect. Fig. 6 shows an exam-  
313 ple of such behavior where the ZTF data and fit show  
314 multiple coherent data point sequences offset from  
315 the best-fit mean model.

- 316 2. Full light curves were inspected for their repeata-  
317 bility between observing seasons (Fig. 7). This  
318 step was sensitive to amplitude modulations with  
319 periods of the order a year or longer.  
320 3. The phased light curves normalized to unit am-  
321 plitude were inspected for their repeatability be-  
322 tween observing seasons. This step was sensitive  
323 to phase modulations of a few percent or larger on  
324 time scales of the order a year or longer. Fig. 8  
325 shows an example of a Blazhko star where season-  
326 to-season phase and amplitude modulations are  
327 seen in both the LINEAR data and (especially)

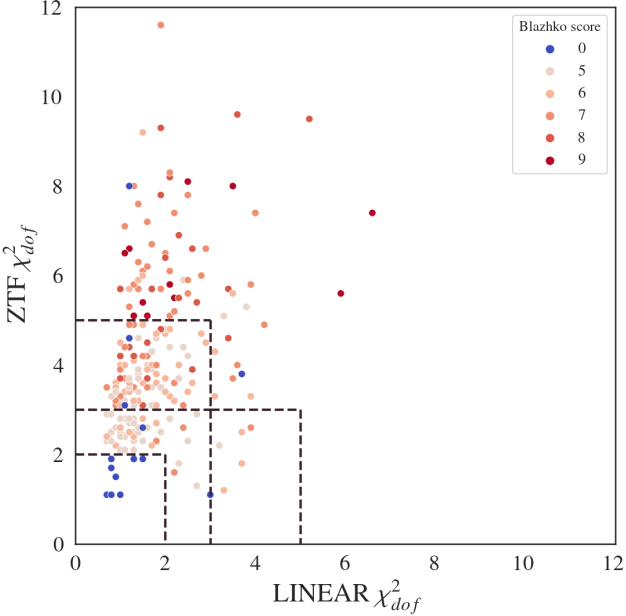


**Figure 5.** Analogous to figure 2, except that here only 228 visually verified Blazhko stars are shown.

the ZTF data. Another example is shown in Fig. 9 where only phase modulation is visible, without any discernible amplitude modulation.

After visually analyzing the starting sample of 531 Blazhko candidates, we visually confirmed expected Blazhko behavior for 228 stars (214 out of 479 and 14 out of 52). LINEAR IDs and other characteristics for confirmed Blazhko stars are listed in Table 1 (Appendix A). Statistical properties of the selected sample of Blazhko stars are discussed in detail in the next section.

#### 4. RESULTS

Starting with a sample of 2857 field RR Lyrae stars with both LINEAR and ZTF data, we constructed a subsample of 1996 with light curves of sufficient quality and selected and verified 228 stars that exhibit convincing Blazhko effect. In this section we compare various statistical properties of selected Blazhko stars to those of the starting sample.

##### 4.1. The Blazhko Incidence Rate

The implied incidence rate for the Blazhko effect is  $11.4 \pm 0.8\%$ . Due to selection effects and unknown completeness, this rate should be considered as a lower limit. When ab and c types are considered separately, the rate is slightly higher for the former than for the latter:  $12.1 \pm 0.9\%$  vs.  $9.2 \pm 1.3\%$ . The difference of  $2.9\%$  has low statistical significance ( $< 2\sigma$ ).

##### 4.2. Period, Amplitude and Magnitude Distributions

Marginal distributions of period, amplitude and apparent magnitude for the starting sample and Blazhko

stars are compared in Fig. 10. Encouragingly, their magnitude distributions are statistically indistinguishable which indicates that the completeness is not a strong function of the photometric signal-to-noise ratio. This result is probably due to the fact that the sample is defined by the depth of LINEAR survey, while ZTF survey is deeper than this limit and its photometric quality is approximately constant across the probed magnitude range.

The suspected differences in amplitude and period distributions are further explored in Fig. 11. It is already discernible by eye that the period distribution for Blazhko stars of ab type is shifted to smaller values than for the starting sample. We have found that the median period for ab type Blazhko stars is about 5% shorter than for the starting RR Lyrae sample. This difference is significant at the  $7.1\sigma$  level. At the same time, the difference in median amplitudes for ab type stars corresponds to only  $0.6\sigma$  deviation. No statistically significant differences are found in period and amplitude distributions for c type stars.

If modulation amplitudes are correlated with periods such that larger modulation amplitudes occur in shorter period RRab stars, and if our selection efficiency is lower for smaller modulation amplitudes, then the detected period shift for ab type Blazhko stars might be at least partially due to combination of these two effects. This possibility does not appear likely. First, as we discussed in preceeding section, our sample is defined by the depth of LINEAR survey, while ZTF survey is significantly deeper than this limit and its photometric quality is approximately constant across the probed magnitude range. Since it is sufficient for a star to display the Blazhko effect only in ZTF to be included in the sample, we do not expect strong selection effects (except for the LINEAR magnitude cutoff of course). Furthermore, Skarka et al. (2020) searched for period - modulation amplitude correlation using a large sample of stars with OGLE measurements and did not find any.

##### 4.3. Long-term behavior of Blazhko Stars

During visual analysis, we noticed that some Blazhko stars exhibit convincing Blazhko effect either in LINEAR or in ZTF data, but not in both surveys. Fig. 12 shows an example where amplitude modulation is clearly seen in LINEAR light curves, while not discernible in ZTF light curves. There are also examples of stars where Blazhko effect is evident in ZTF but not in LINEAR data (e.g., LINEARid = 19466437, 14155360). This finding strongly suggests that Blazhko effect can appear and disappear on time scales shorter than about a decade.

#### 5. DISCUSSION AND CONCLUSIONS

We found excellent agreement between the best-fit periods for RR Lyrae stars estimated separately from LINEAR and ZTF light curves. Only one star in our sam-

## STAR 1140 from 2857

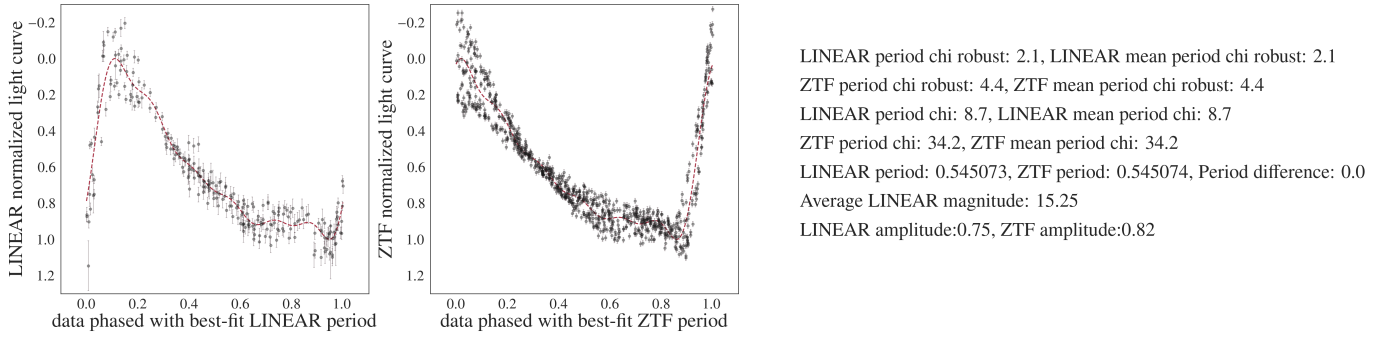


**Figure 6.** An illustration of visual analysis of phased light curves for the selected Blazhko candidates. The left panel shows LINEAR data and the right panel shows ZTF data (symbols with “error bars”) for star with LINEARid = 10030349. The dashed lines are best-fit models. The numbers listed on the right side were added to aid visual analysis. Note multiple coherent data point sequences offset from the best-fit mean model in the right panel.

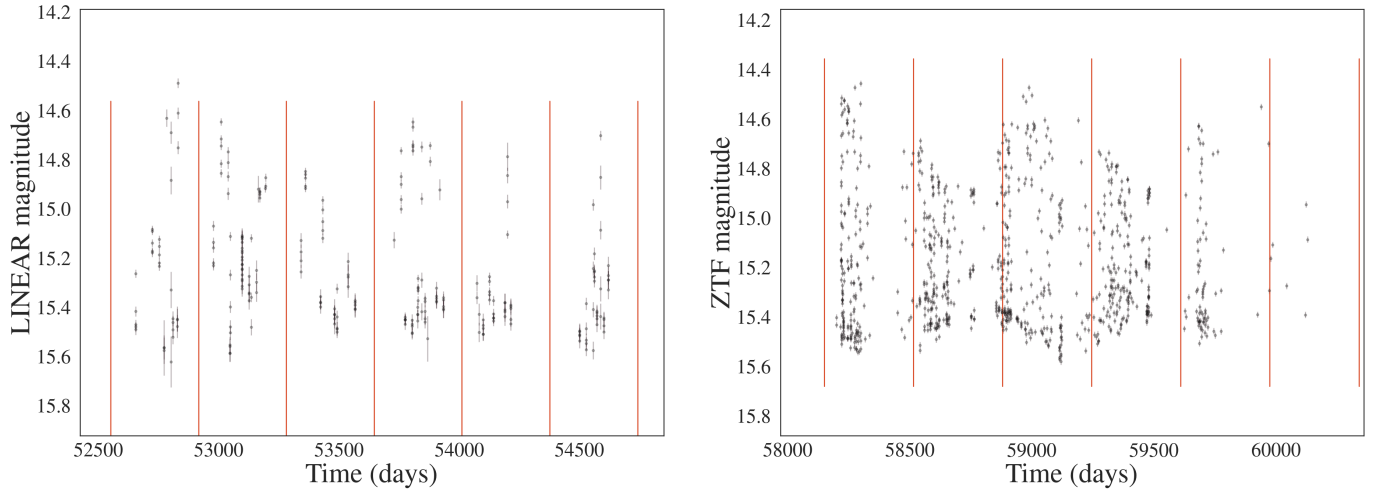


**Figure 7.** An illustration of visual analysis of full light curves for the selected Blazhko candidates with emphasis on their repeatability between observing seasons, marked with vertical lines (left: LINEAR data; right: ZTF data). Data shown are for star with LINEARid = 10030349. Note strong amplitude modulation between observing seasons.

ple (CT CrB, LINEARid=17919686), was previously reported as a Blazhko star (Skarka 2013). The sample of 228 stars presented here increases the number of field RR Lyrae stars displaying the Blazhko effect by more than 50% and places a lower limit of  $(11.4 \pm 0.8)\%$  for their incidence rate. The reported incidence rates for the Blazhko effect range from 5% (Szczygieł & Fabrycky 2007) to 60% (Szabó et al. 2014). Differences in reported incidence rates can occur due to varying data precision, the temporal baseline length, and differences in visual or algorithmic analysis. For a relatively small sample of 151 stars with Kepler data, a claim has been made that essentially every RR Lyrae star exhibits modulated light curve (Kovacs 2018). The difference in Blazhko incidence rates for the two most extensive samples, obtained by the OGLE-III survey for the Large Magellanic Cloud (LMC, 20% out of 17,693 stars; Soszyński et al. 2009) and the Galactic bulge (30% out of 11,756 stars;

Soszyński et al. 2011) indicates a possible variation of the Blazhko incidence rate with underlying stellar population properties.

We find that ab type RR Lyrae which show the Blazhko effect have about 5% (0.030 day) shorter periods than starting sample. While not large, the statistical significance of this difference is  $7.1\sigma$ . At a similar uncertainty level ( $\sim 1\%$ ), we don’t detect period difference for c type stars, and don’t detect any difference in amplitude distributions. We also find that for some stars the Blazhko effect is discernible in only one dataset. This finding strongly suggests that Blazhko effect can appear and disappear on time scales shorter than about a decade, in agreement with literature (Jurcsik et al. 2009; Poretti et al. 2010; Benkő et al. 2014).

The LINEAR and ZTF datasets analyzed in this work were sufficiently large that we had to rely on algorithmic pruning of the initial sample. The sample size problem

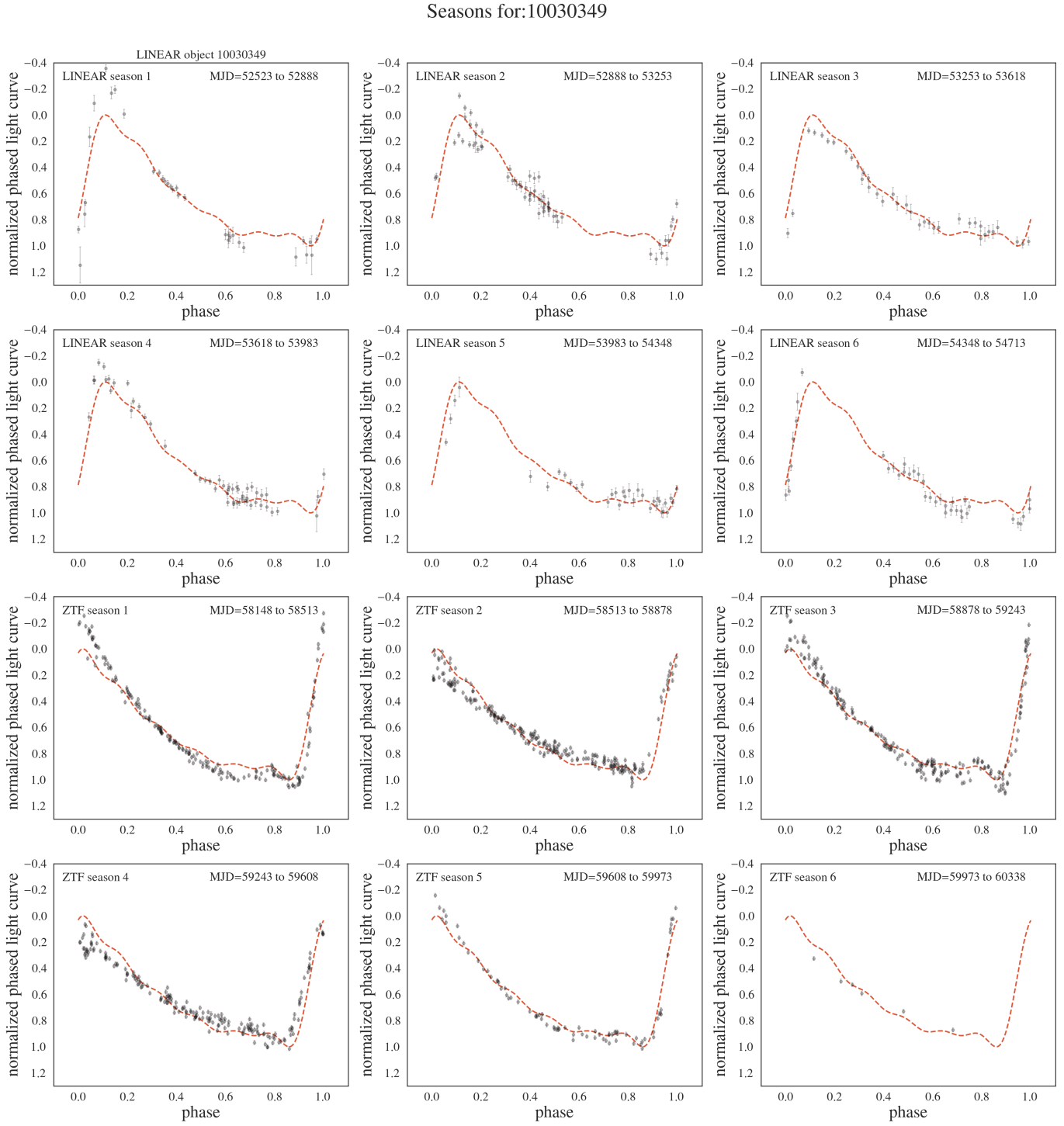


**Figure 8.** The phased light curves normalized to unit amplitude of the overall best-fit model are shown for single observing seasons and compared to the mean best-fit models (top six panels: LINEAR data; bottom six panels: ZTF data). Data shown are for star with LINEARid = 10030349. Season-to-season phase and amplitude modulations are seen in both the LINEAR and the ZTF data.

will be even larger for surveys such as the Legacy Survey of Space and Time (LSST; Ivezić et al. 2019). LSST will be an excellent survey for studying Blazhko effect (Hernitschek & Stassun 2022) because it will have both a long temporal baseline (10 years) and a large number of observations per object (nominally 825; LSST Science Requirements Document<sup>4</sup>). We anticipate a higher fraction of discovered Blazhko stars with LSST than reported here due to better sampling and superior photometric quality, since the incidence rate of the Blazhko effect increases with sensitivity to small-amplitude modulation, and thus with photometric data quality (Jurcsik et al. 2009).

The size and quality of LSST sample will motivate further developments of the selection algorithms. One obvious improvement will be inspection of neighboring objects to confirm photometric quality, as well as inspection of images to test implication of an isolated point source (e.g., blended object photometry can be affected by variable seeing beyond aperture correction valid for isolated point sources). Another improvement is forward modeling of the Blazhko modulation, rather than searching for  $\chi^2$  outliers (Benkő et al. 2011; Guggenberger et al. 2012). For example, Skarka et al. (2020) classified Blazhko stars in 6 classes using the morphology of their amplitude modulation (the most dominant class includes 90% of the sample). They also found bimodal distribution of Blazhko periods, with two components centered on 48 d and 186 d. These results give hope that forward modeling of the Blazhko effect will improve the selection of such stars.

We thank Mathew Graham for providing *ztfquery* code example to us, and Robert Szabó for expert comments that improved presentation.

Ž.I. acknowledges funding by the Fulbright Foundation and thanks the Ruđer Bošković Institute (Zagreb, Croatia) for hospitality.

Based on observations obtained with the Samuel Oschin Telescope 48-inch and the 60-inch Telescope at the Palomar Observatory as part of the Zwicky Transient Facility project. ZTF is supported by the National Science Foundation under Grants No. AST-1440341 and AST-2034437 and a collaboration including current partners Caltech, IPAC, the Weizmann Institute of Science, the Oskar Klein Center at Stockholm University, the University of Maryland, Deutsches Elektronen-Synchrotron and Humboldt University, the TANGO Consortium of Taiwan, the University of Wisconsin at Milwaukee, Trinity College Dublin, Lawrence Livermore National Laboratories, IN2P3, University of Warwick, Ruhr University Bochum, Northwestern University and former partners the University of Washington, Los Alamos National Laboratories, and Lawrence Berkeley National Laboratories. Operations are conducted by COO, IPAC, and UW.

The LINEAR program is funded by the National Aeronautics and Space Administration at MIT Lincoln Laboratory under Air Force Contract FA8721-05-C-0002. Opinions, interpretations, conclusions and recommendations are those of the authors and are not necessarily endorsed by the United States Government.

*Software:* Astropy (Astropy Collaboration et al. 2018, 2022), Matplotlib (Hunter 2007), SciPy (Virtanen et al. 2020), astroML (VanderPlas et al. 2012)

## APPENDIX

Table 1: The first 10 confirmed Blazhko stars with their LINEAR IDs in the first column and then, for both LINEAR and ZTF, their computed light curve periods (day), the number of data points per light curve, robust and ordinary  $\chi^2$  values, and light curve amplitudes, followed by amplitude difference between LINEAR and ZTF, the strength and period of Blazhko peaks in their periodograms, light curve type (1: ab, 2: c), detection significance flag for the periodograms (Z, L or “-” for no detection; the strength and period of Blazhko peaks are not reliable when “-”) and the selection score (see Sections 3.1 and 3.2 for details). The full table is available in online edition.

<sup>4</sup> Available as ls.st/srd

## Seasons for:16300450

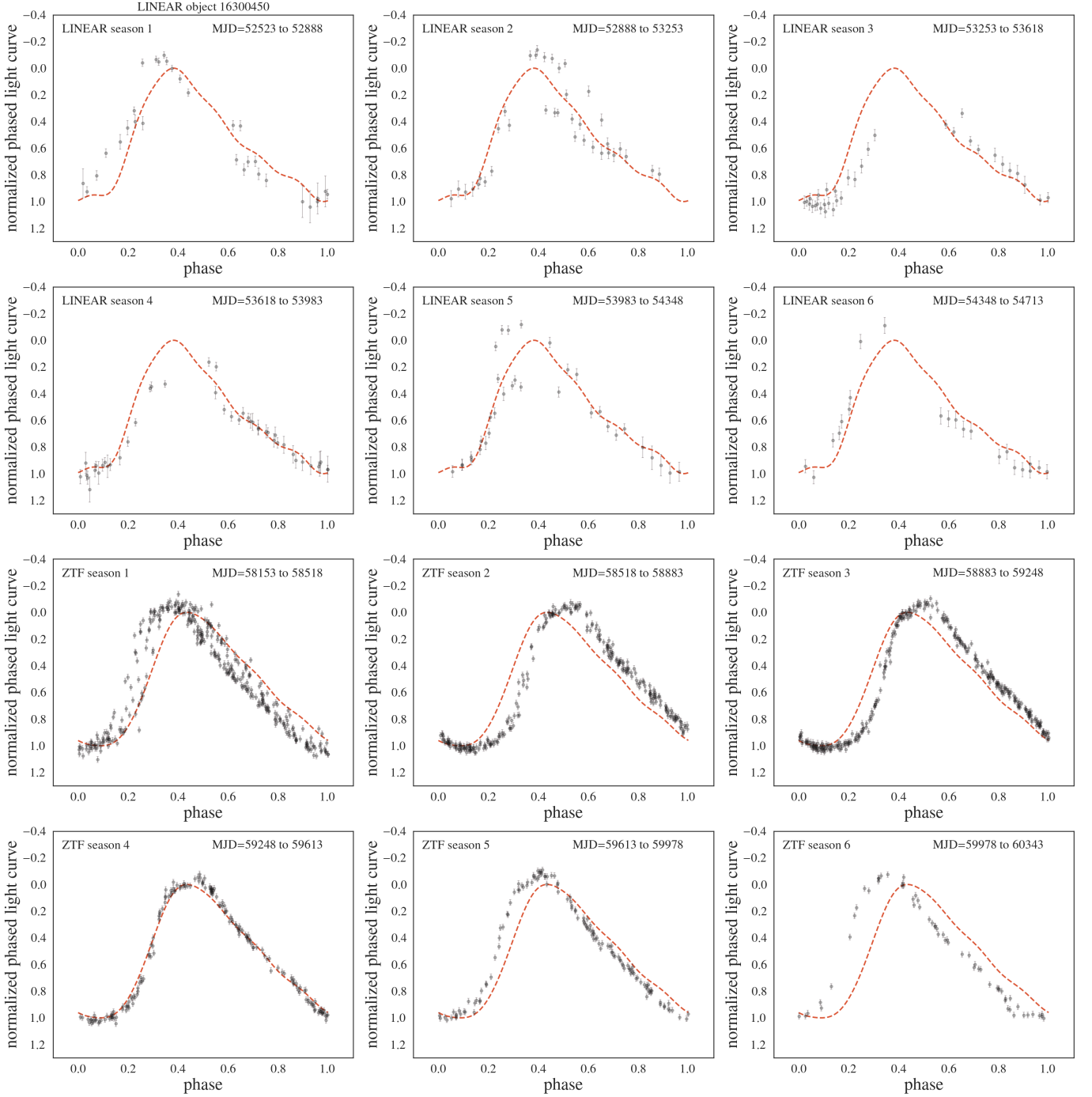


**Figure 9.** Analogous to Fig. 8, except that star with LINEARid = 16300450 is shown. Unlike example shown in Fig. 8, only phase modulation is visible here, without any amplitude modulation, in both LINEAR and ZTF light curves.

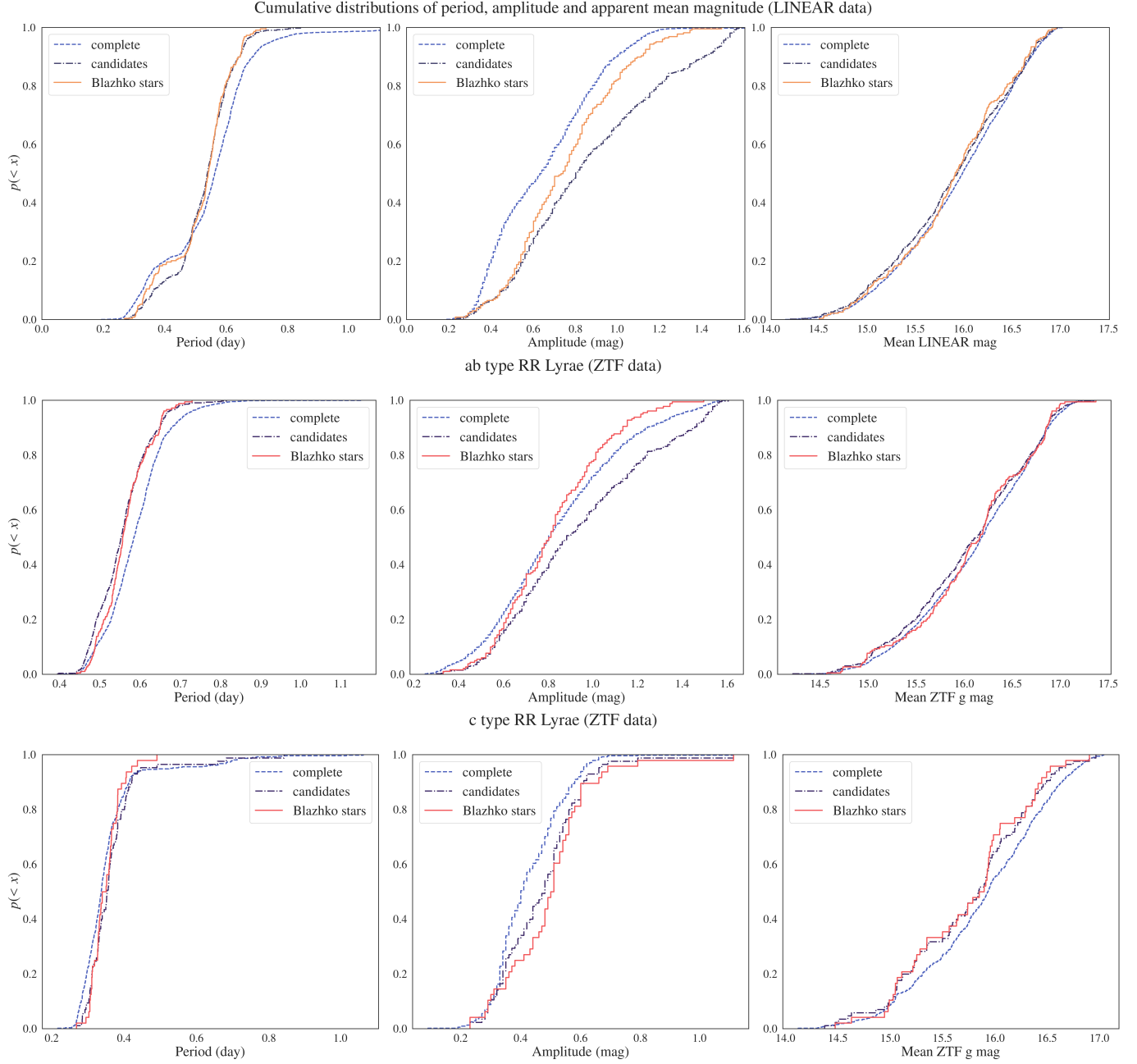


**Figure 10.** A comparison of cumulative distributions of period (left), amplitude (middle) and apparent magnitude for starting sample, selected Blazhko candidates and visually verified Blazhko stars. The top row is based on LINEAR data and both ab type and c type stars. The middle and bottom rows are based on ZTF data, and show separately data for ab type and c type stars, respectively. The differences in period and amplitude distributions are further examined in figure 11.

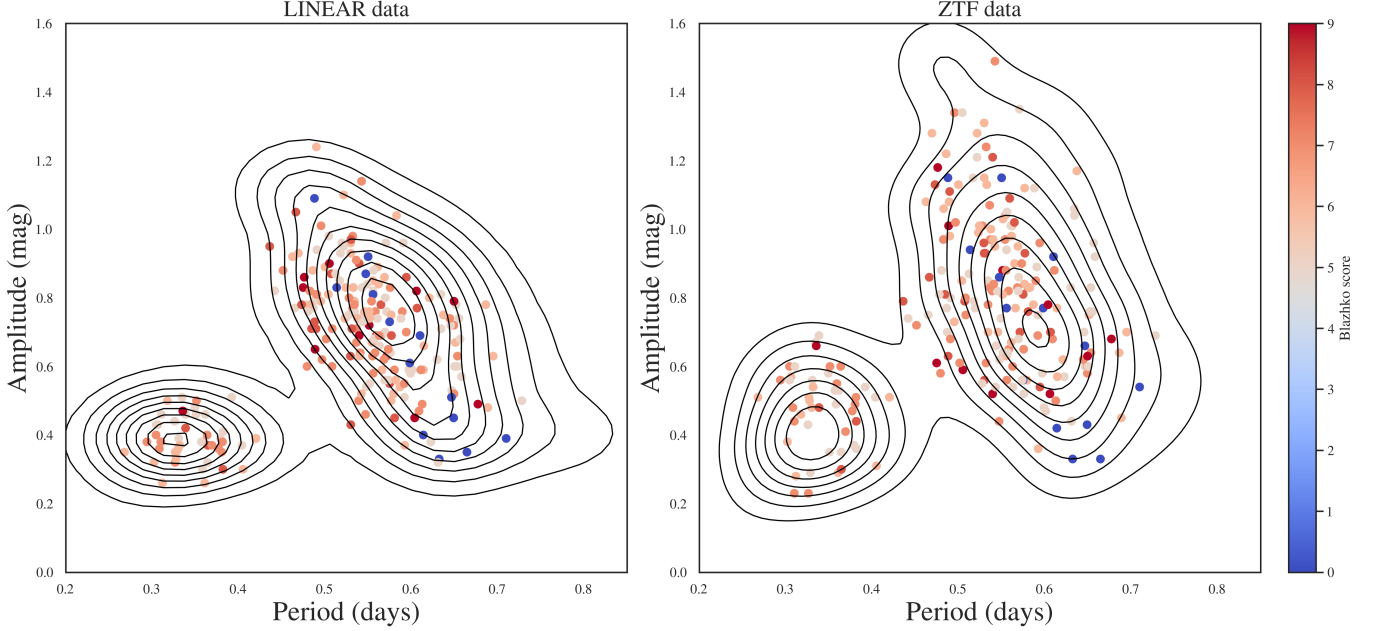


**Figure 11.** Comparison of amplitude–period distributions (the Bailey diagram) for the starting sample of 1,996 RR Lyrae stars (contours) and 228 selected candidate Blazhko stars (symbols). The clump in the lower left corresponds to c type RR Lyrae and the other one to ab type. Note that the period distribution for ab type Blazhko stars is shifted left (by about 0.03 day, or 5%).

519

LID	P <sub>L</sub>	P <sub>Z</sub>	N <sub>L</sub>	N <sub>Z</sub>	χ <sub>L,r</sub> <sup>2</sup>	χ <sub>Z,r</sub> <sup>2</sup>	χ <sub>L</sub> <sup>2</sup>	χ <sub>Z</sub> <sup>2</sup>	A <sub>L</sub>	A <sub>Z</sub>	δA	Bp <sub>L</sub>	Bp <sub>Z</sub>	Bp <sub>L</sub>	Bp <sub>Z</sub>	t	f	B <sub>s</sub>	B <sub>f</sub>
158779	0.609207	0.609189	293	616	1.6	3.9	3.7	34.2	0.47	0.68	0.21	1.6443	1.6444	352.7337	350.2	1	-	7	1
263541	0.558218	0.558221	270	503	2.9	6.6	15.8	110.4	0.64	0.82	0.18	1.8621	1.8025	14.1513	89.9	1	-	7	1
393084	0.530027	0.530033	493	372	1.1	3.2	1.6	19.2	0.96	1.31	0.35	1.9447	1.8896	17.2369	347.2	1	-	6	1
810169	0.465185	0.465212	289	743	2.1	2.8	6.0	15.1	0.77	0.75	0.02	2.2232	2.2230	13.6017	13.6	1	-	5	1
924301	0.507503	0.507440	418	189	1.9	9.3	13.8	162.9	0.87	0.79	0.08	2.0043	1.9763	29.5072	178.4	1	-	8	1
970326	0.592233	0.592231	275	552	1.1	2.1	1.9	7.7	0.51	0.75	0.24	1.7563	1.6992	14.7656	93.2	1	-	5	1
999528	0.658401	0.658407	564	213	1.2	2.7	1.8	21.7	0.57	0.92	0.35	1.5527	1.5510	29.5247	31.0	1	-	5	1
1005497	0.653607	0.653605	607	192	1.1	2.1	2.1	12.4	0.60	0.83	0.23	1.5639	1.5481	29.4638	55.1	1	-	5	1
1092244	0.649496	0.649558	590	326	1.2	3.6	2.3	32.1	0.72	0.58	0.14	1.5735	1.5640	29.5421	40.8	1	-	7	1
1240665	0.632528	0.632522	468	311	3.0	1.1	25.2	1.6	0.33	0.33	0.00	1.6149	1.5865	29.4942	182.3	1	Z	0	2

520

## REFERENCES

- 521 Alcock, C., Alves, D. R., Becker, A., et al. 2003, ApJ, 598,  
522 597, doi: [10.1086/378689](https://doi.org/10.1086/378689)
- 523 Astropy Collaboration, Price-Whelan, A. M., Sipőcz, B. M.,  
524 et al. 2018, AJ, 156, 123, doi: [10.3847/1538-3881/aabc4f](https://doi.org/10.3847/1538-3881/aabc4f)
- 525 Astropy Collaboration, Price-Whelan, A. M., Lim, P. L.,  
526 et al. 2022, ApJ, 935, 167, doi: [10.3847/1538-4357/ac7c74](https://doi.org/10.3847/1538-4357/ac7c74)
- 527 Bellm, E. C., Kulkarni, S. R., Graham, M. J., et al. 2019,  
528 PASP, 131, 018002, doi: [10.1088/1538-3873/aaecbe](https://doi.org/10.1088/1538-3873/aaecbe)
- 529 Benkő, J. M., Plachy, E., Szabó, R., Molnár, L., & Kolláth,  
530 Z. 2014, ApJS, 213, 31, doi: [10.1088/0067-0049/213/2/31](https://doi.org/10.1088/0067-0049/213/2/31)
- 531 Benkő, J. M., Szabó, R., & Paparó, M. 2011, MNRAS, 417,  
532 974, doi: [10.1111/j.1365-2966.2011.19313.x](https://doi.org/10.1111/j.1365-2966.2011.19313.x)
- 533 Benkő, J. M., Kolenberg, K., Szabó, R., et al. 2010,  
534 MNRAS, 409, 1585,  
535 doi: [10.1111/j.1365-2966.2010.17401.x](https://doi.org/10.1111/j.1365-2966.2010.17401.x)
- 536 Blažkó, S. 1907, Astronomische Nachrichten, 175, 325,  
537 doi: [10.1002/asna.19071752002](https://doi.org/10.1002/asna.19071752002)
- 538 Catelan, M. 2009, Ap&SS, 320, 261,  
539 doi: [10.1007/s10509-009-9987-8](https://doi.org/10.1007/s10509-009-9987-8)
- 540 Guggenberger, E., Kolenberg, K., Nemec, J. M., et al. 2012,  
541 MNRAS, 424, 649, doi: [10.1111/j.1365-2966.2012.21244.x](https://doi.org/10.1111/j.1365-2966.2012.21244.x)
- 542 Hernitschek, N., & Stassun, K. G. 2022, ApJS, 258, 4,  
543 doi: [10.3847/1538-4365/ac3baf](https://doi.org/10.3847/1538-4365/ac3baf)
- 544 Hunter, J. D. 2007, Computing in Science & Engineering, 9,  
545 90, doi: [10.1109/MCSE.2007.55](https://doi.org/10.1109/MCSE.2007.55)

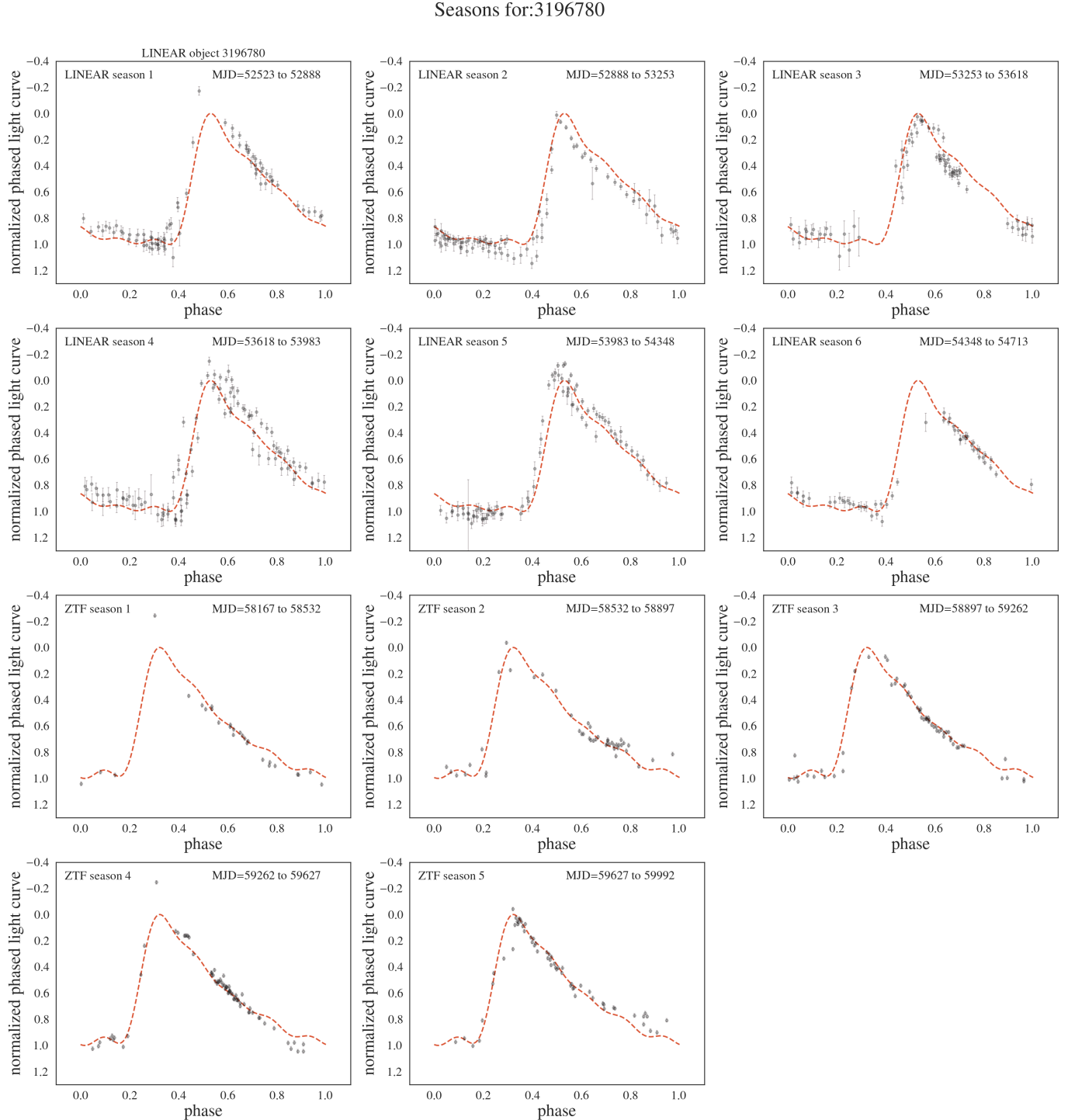


**Figure 12.** Analogous to Fig. 8, except that star with LINEARid = 3196780 is shown. Amplitude modulation is clearly seen in LINEAR light curves (top two rows), while not discernible in ZTF light curves (bottom two rows). Additional stars with similar behavior include LINEARid = 2889542, 7723614, 8342007. This behavior strongly suggests that Blazhko effect can appear and disappear on time scales shorter than about a decade.

- <sup>546</sup> Ivezić, Ž., Kahn, S. M., Tyson, J. A., et al. 2019, ApJ, 873,  
<sup>547</sup> 111, doi: [10.3847/1538-4357/ab042c](https://doi.org/10.3847/1538-4357/ab042c)
- <sup>548</sup> Jurcsik, J., Sódor, Á., Szeidl, B., et al. 2009, MNRAS, 400,  
<sup>549</sup> 1006, doi: [10.1111/j.1365-2966.2009.15515.x](https://doi.org/10.1111/j.1365-2966.2009.15515.x)
- <sup>550</sup> Kolenberg, K. 2008, in Journal of Physics Conference  
<sup>551</sup> Series, Vol. 118, Journal of Physics Conference Series  
<sup>552</sup> (IOP), 012060, doi: [10.1088/1742-6596/118/1/012060](https://doi.org/10.1088/1742-6596/118/1/012060)
- <sup>553</sup> Kovács, G. 2009, in American Institute of Physics  
<sup>554</sup> Conference Series, Vol. 1170, Stellar Pulsation:  
<sup>555</sup> Challenges for Theory and Observation, ed. J. A. Guzik  
<sup>556</sup> & P. A. Bradley, 261–272, doi: [10.1063/1.3246458](https://doi.org/10.1063/1.3246458)
- <sup>557</sup> Kovacs, G. 2016, Communications of the Konkoly  
<sup>558</sup> Observatory Hungary, 105, 61,  
<sup>559</sup> doi: [10.48550/arXiv.1512.05722](https://doi.org/10.48550/arXiv.1512.05722)
- <sup>560</sup> —. 2018, A&A, 614, L4, doi: [10.1051/0004-6361/201833181](https://doi.org/10.1051/0004-6361/201833181)
- <sup>561</sup> Mizerski, T. 2003, AcA, 53, 307,  
<sup>562</sup> doi: [10.48550/arXiv.astro-ph/0401612](https://doi.org/10.48550/arXiv.astro-ph/0401612)
- <sup>563</sup> Palaversa, L., Ivezić, Ž., Eyer, L., et al. 2013, AJ, 146, 101,  
<sup>564</sup> doi: [10.1088/0004-6256/146/4/101](https://doi.org/10.1088/0004-6256/146/4/101)
- <sup>565</sup> Poretti, E., Paparó, M., Deleuil, M., et al. 2010, A&A, 520,  
<sup>566</sup> A108, doi: [10.1051/0004-6361/201014941](https://doi.org/10.1051/0004-6361/201014941)
- <sup>567</sup> Prudil, Z., & Skarka, M. 2017, MNRAS, 466, 2602,  
<sup>568</sup> doi: [10.1093/mnras/stw3231](https://doi.org/10.1093/mnras/stw3231)
- <sup>569</sup> Sesar, B., Stuart, J. S., Ivezić, Ž., et al. 2011, AJ, 142, 190,  
<sup>570</sup> doi: [10.1088/0004-6256/142/6/190](https://doi.org/10.1088/0004-6256/142/6/190)
- <sup>571</sup> Sesar, B., Ivezić, Ž., Grammer, S. H., et al. 2010, ApJ, 708,  
<sup>572</sup> 717, doi: [10.1088/0004-637X/708/1/717](https://doi.org/10.1088/0004-637X/708/1/717)
- <sup>573</sup> Sesar, B., Ivezić, Ž., Stuart, J. S., et al. 2013, AJ, 146, 21,  
<sup>574</sup> doi: [10.1088/0004-6256/146/2/21](https://doi.org/10.1088/0004-6256/146/2/21)
- <sup>575</sup> Skarka, M. 2013, A&A, 549, A101,  
<sup>576</sup> doi: [10.1051/0004-6361/201220398](https://doi.org/10.1051/0004-6361/201220398)
- <sup>577</sup> Skarka, M., Prudil, Z., & Jurcsik, J. 2020, MNRAS, 494,  
<sup>578</sup> 1237, doi: [10.1093/mnras/staa673](https://doi.org/10.1093/mnras/staa673)
- <sup>579</sup> Smith, H. A. 1995, Cambridge Astrophysics Series, 27
- <sup>580</sup> Soszyński, I., Udalski, A., Szymański, M. K., et al. 2010,  
<sup>581</sup> AcA, 60, 165, doi: [10.48550/arXiv.1009.0528](https://doi.org/10.48550/arXiv.1009.0528)
- <sup>582</sup> —. 2009, AcA, 59, 1, doi: [10.48550/arXiv.0903.2482](https://doi.org/10.48550/arXiv.0903.2482)
- <sup>583</sup> Soszyński, I., Dziembowski, W. A., Udalski, A., et al. 2011,  
<sup>584</sup> AcA, 61, 1, doi: [10.48550/arXiv.1105.6126](https://doi.org/10.48550/arXiv.1105.6126)
- <sup>585</sup> Szabó, R. 2014, in IAU Symposium, Vol. 301, Precision  
<sup>586</sup> Asteroseismology, ed. J. A. Guzik, W. J. Chaplin,  
<sup>587</sup> G. Handler, & A. Pigulski, 241–248,  
<sup>588</sup> doi: [10.1017/S1743921313014397](https://doi.org/10.1017/S1743921313014397)
- <sup>589</sup> Szabó, R., Benkő, J. M., Paparó, M., et al. 2014, A&A,  
<sup>590</sup> 570, A100, doi: [10.1051/0004-6361/201424522](https://doi.org/10.1051/0004-6361/201424522)
- <sup>591</sup> Szczygieł, D. M., & Fabrycky, D. C. 2007, MNRAS, 377,  
<sup>592</sup> 1263, doi: [10.1111/j.1365-2966.2007.11678.x](https://doi.org/10.1111/j.1365-2966.2007.11678.x)
- <sup>593</sup> Vanderplas, J. 2015, gatspy: General tools for Astronomical  
<sup>594</sup> Time Series in Python, v0.1.1, Zenodo,  
<sup>595</sup> doi: [10.5281/zenodo.14833](https://doi.org/10.5281/zenodo.14833)
- <sup>596</sup> VanderPlas, J., Connolly, A. J., Ivezić, Z., & Gray, A.  
<sup>597</sup> 2012, in Proceedings of Conference on Intelligent Data  
<sup>598</sup> Understanding (CIDU, 47–54,  
<sup>599</sup> doi: [10.1109/CIDU.2012.6382200](https://doi.org/10.1109/CIDU.2012.6382200)
- <sup>600</sup> Virtanen, P., Gommers, R., Oliphant, T. E., et al. 2020,  
<sup>601</sup> Nature Methods, 17, 261, doi: [10.1038/s41592-019-0686-2](https://doi.org/10.1038/s41592-019-0686-2)